TECHNICAL MEMORANDUM

38

Winter and summer circulation statistics based on ECMWF operational analyses and forecasts

H. Sävijärvi

Research Department

July 1981

European Centre for Medium-Range Weather Forecasts
Europäisches Zentrum für mittelfristige Wettervorhersage
Centre européen pour les prévisions météorologiques à moyen

ABSTRACT

Zonal mean cross sections of temperature, wind and meridional and vertical eddy transports of temperature, humidity and momentum are presented for winter (December 1979 - February 1980) and summer (June - August 1980), based on ECMWF operational global initialized analyses and forecasts at day 10. The operational analyses (data on σ-levels) give statistics similar to the FGGE IIIb ECMWF analyses and in general slightly stronger eddy transports than e.g. in Newell et al (1972). The model day 10 climate is colder, more zonal and has stronger vertical large-scale eddy transports, especially in the tropics where initialization reduces the analysed mean meridional circulation and eddy vertical motions.

1. INTRODUCTION

The purpose of this paper is to document briefly some traditional zonally averaged general circulation statistics for (Northern hemisphere) winter and summer seasons, as given by the ECMWF global analysis-forecasting system during its first year of operations. The results may be considered as reference against which new experiments in the analysis-initialization sequence and/or forecasts can be judged. These winter-summer statistics are presented also for the sake of comparison with similar investigations (but on pressure level data) e.g. Oort and Rasmusson (1971), Newell et al (1972), Rosen and Salstein (1980, NMC analyses and station data) and Kanamitsu (1980, FGGE IIIb analyses). A more complete climatology, based on wave number decomposition on pressure level data, will be reported later. The present calculations are based on data on the staggered ECMWF model N48 grid on 15 σ-levels. While the comparison to statistics based on pressure level data is thus not formally valid, the two approaches have given almost identical results for shorter time periods (ECMWF/SAC (81) 8).

The analyzed data has been initialized with the adiabatic nonlinear normal mode method (Temperton and Williamson, 1979). This method reduces the mean meridional circulation considerably in the tropics (Temperton, 1980) and is likely to affect also the eddy vertical motion in the tropics. The mean meridional circulation and vertical eddy fluxes are thus, unfortunately, artificially weak in the tropics in the initialized-analyzed data.

2. WINTER AND SUMMER PERIOD ZONAL AVERAGES

Some zonally averaged atmospheric circulation statistics are presented averaged over the 3-month periods December 1979 - February 1980 and June - August 1980. The data has been taken from ECMWF operational analyses after normal mode initialization, and the grid point data on 15 σ-levels has been used. The data "levels" thus unconventionally follow the terrain over the mountain peaks but, on the other hand, the boundary layer structure is well represented with three levels within it. In plotting the cross sections, however, pressure has been used as vertical coordinate. The same statistics are also presented using the ECMWF forecast ensemble for day 10 during the three winter and three summer months. Because the main features of the

statistics presented are well-known since the work of Oort and Rasmusson (1971), Newell et al (1972) and others, mainly the deviations from previously known features will be discussed.

Fig. 1 shows the temperature distribution $[\bar{T}]$, which is rather similar to Newell et al (1972) with large seasonal stratospheric temperature variation over the South Pole. In the forecast data, the temperature has decreased a few degrees in both hemispheres, except near the ground. This is probably due to the parameterization of physical processes in the model; net cooling through simulated radiation is systematically stronger than heating through simulated condensation and turbulent processes, especially at the beginning of the forecast.

The zonal wind field is in Fig. 2. The distribution of $[\bar{u}]$ is very similar to the FGGE period winter 1978-1979 and summer 1979 statistics (Kanamitsu, 1980, and personal communication) based on ECMWF non-initialized analyses from FGGE IIb large data set. The zonal jet maxima are somewhat stronger than in Newell et al (1972). In the boundary layer the easterly wind maximum in the winter hemisphere tropics is similar to Newell et al (1972) but not to Kanamitsu (1980). These two references display weak easterly polar winter surface winds not found in the present data.

The southern hemisphere stratospheric polar night jet maximum at 60^{o}S supports the finding of Kanamitsu that this jet far exceeds the reported values (45 m/s at 20 mb, 60^{o} S) in Newell et al (1972). The top level in the present data is about 25 mb and the jet maximum values at that level (60 m/s) are similar in the present operational analyses to the FGGE IIIb analyses.

The zonal wind fields from the day 10 forecast ensemble show, when compared to the analyzed values, a slight poleward and upward shift in the position of the main jets, increased zonal wind speeds at latitudes $30-50^{o}$ and weaker zonal winds in the polar regions. In the summer hemisphere, the jet structure is latitudinally narrower and the tropical upper troposphere easterlies stronger and more extended in the forecasts than in the analyzed data.

The zonally averaged meridional wind field $[\bar{v}]$ is in Fig. 3. In the non-initialized ECMWF FGGE analyses, the 3-cell structure is preserved well (Kanamitsu, 1980), but the tropical Hadley cell is largely diminished in the initialized data as seen in Fig. 3. Since the tropical rising motion is

typically caused by non-adiabatically driven deep convection, the adiabatic normal mode initialization used in ECMWF during 1980 did not maintain it. This is a serious drawback for diagnostic studies because all the zonally averaged meridional and vertical fluxes $[\overline{sv}]$, $[\overline{s\omega}]$ are underestimated in the initialized data as a result. In the following, therefore, only the eddy parts of meridional and vertical fluxes $[\overline{sv}] - [\bar{s}][\bar{v}]$, $[\overline{s\omega}] - [\bar{s}][\bar{\omega}]$ are shown; this includes the effect of both standing and transient eddies. A similar but even more complete elimination of meridional overturnings takes place in the NMC Hough analyses, as discussed in Rosen and Salstein (1980).

The mean meridional circulation is quickly recovered in the model and the day 10 forecast $[\bar{v}]$ -field is quite realistic compared to the station data estimates of Rosen and Salstein (1980) and Oort and Rasmusson (1971), and non-initialized ECMWF analyses.

The meridional angular momentum flux $[\overline{uv}]$ is essentially maintaining the zonally averaged jets against frictional dissipation and is therefore one of the key quantities in general circulation. Its estimation is known to be sensitive to data material (Arpe, 1980). Fig. 4 gives the eddy part $[\overline{uv}] - [\bar{u}][\bar{v}] = [\bar{u}^*\bar{v}^*] + [\overline{u'v'}]$ (standing and transient) of this flux; the eddy flux dominates the total flux outside the tropical Hadley cell where the mean meridional flux $[\bar{u}][\bar{v}]$ gives a sizeable contribution. The general features of the eddy flux pattern agree again well with the FGGE analysed data except that the southward eddy flux at 60° N is stronger in the FGGE winter material than in the present data and many earlier results; Kanamitsu (1980) shows that these large values arose from standing eddies and suggests that they may be due to the blocking wave pattern during winter 1979.

The maximum eddy transport values in the winter hemisphere jet area are slightly larger in this data than in other studies. The cross-equatorial eddy transport of angular momentum near the tropopause, from winter to summer hemisphere, exists in this data, but is much weaker than in Newell et al (1972), where it was largely coming from the transient part. However, both in Kanamitsu (1980) and Rosen and Salstein (1980), this transient equatorial flux maximum is very weak and the total eddy flux more in line with the present results.

Fig. 5 shows the meridional transport of temperature in large-scale eddies $[\bar{T}^*\bar{v}^*] + [\overline{T'v'}]$. Exceptions to previous results in this well-documented field (e.g. Oort and Rasmusson (1972), Newell et al (1974), Rosen and Salstein (1980)) are the vertically more extended northward eddy heat flux in the upper troposphere during northern hemisphere winter, and the strong poleward heat flux at 75° S, 500 mb, which exists during both seasons. The convergence of this heat flux may help to maintain the relatively high Antarctic tropospheric temperatures seen in Fig. 1.

The day 10 forecast climate is notably distorted in the boundary layer eddy heat flux. The same happens to the meridional transport of humidity in large-scale eddies in the forecasts, Fig. 6. In the analysed data, the humidity eddy flux is nearly symmetric about the equator except in the summer hemisphere trade wind region, where a strong poleward eddy flux is found. This feature is exaggerated in the model data.

The zonally averaged vertical transports of temperature s = T, humidity s = q and momentum s = u , in large-scale eddies $[\bar{s}^*\bar{\omega}^*] + [\overline{s'\omega'}]$ are documented in Figs. 7, 8 and 9 respectively, with ω calculated in each grid point from the initialized large-scale vertically integrated wind divergence:

$$\omega = \sigma \underline{v} \cdot \nabla_\sigma p_s - \int_0^\sigma \nabla_\sigma \cdot (p_s \underline{v}) \, d\sigma$$

Maps of vertical velocity so obtained have been shown by Cats and Tracton (1980) to be in good agreement with the solution of the quasi-geostrophic ω equation below 300 mb, if the analyses have been initialized by the non-linear normal mode method, as expected from Leith's work (1980).

The vertical eddy transport of temperature (Fig. 7) is generally upward and has its maximum in the winter hemisphere mid-latitude mid-troposphere. An upward local transport occurs near the South pole analogous to the poleward transport in Fig. 5. The model data reproduces the gross features of the analysed transport, but is more effective in the upward eddy heat transport.

In the maintenance of the zonally and time averaged temperature $[\bar{T}]$ the eddy vertical heat flux enters through the convergence of the flux and also through the conversion of energy between kinetic energy and sensible heat in large scale eddies:

$$(-\frac{\partial}{\partial p} + \frac{R}{C_p p}) \; ([\bar{T}^*\bar{\omega}^*] + [\overline{T'\omega'}])$$

Based on the values in Fig. 7, the conversion term is mainly negative but only about -0.1° C/day while the vertical eddy flux convergence is generally positive in the upper troposphere and negative in the lower troposphere, and is about 0.4° C in absolute values in winter mid-latitudes, where its maximum is.

The total horizontal and vertical heat transports are determined by the heating distribution in the time mean, and in reverse the analysed transports could be used to return the heating distribution. Because the mean meridional transport parts $[\bar{T}][\bar{v}],[\bar{T}][\bar{\omega}]$ and therefore also the total fluxes are underestimated in the tropics at present, due to the initialization, this indirect calculation of the zonal mean diabatic heating field is not attempted here.

Fig. 8 gives the vertical eddy transport of moisture. The mid-latitude large-scale eddies are effectively transporting moisture upward as well as temperature, maximum transport occurring at 700 mb level. The ECMWF forecast is even more active having transports exceeding the analysed values by 50%. Moreover, in the tropical lower troposphere, where the synoptic scale vertical eddy humidity transport is small in the analysed data (most of the transport taking place in sub-synoptic convective phenomena), the model-produced data exhibits large synoptic-scale eddy upward transport, except very near the ground, where a systematic downward eddy humidity transport exists, mainly in the summer hemisphere.

Fig. 9 shows the vertical eddy momentum flux $[\bar{u}^{*}\bar{\omega}^{*}] + [\overline{u'\omega'}]$ for completeness, although the convergence of this flux is in general much smaller than the convergence of the meridional flux (in Fig. 4) and the term less important in the maintenance of the zonal mean wind. Its pattern is more stable to seasonal variations in the southern hemisphere and in the forecasts. The eddy flux is upwards in subtropics, towards higher zonal velocities. Thus the vertical eddy flux of momentum is against thegradient of the mean angular velocity in the subtropical troposphere, just as the meridional eddy flux.

Compared to the analyses, the upward subtropical eddy momentum flux is stronger in the forecasts and its maximum is situated on the poleward side of the winter hemisphere jet. The vertical convergence of the flux is thus acting to increase zonal wind poleward from the jet; this could be related to the observed poleward shift of the jet locations in the forecasts.

REFERENCES

Arpe, K. 1980 Confidence limits for vertification and energetics studies. ECMWF Technical Report No. 18, pp. 24

Cats, G. and Tracton, S. 1980 Two case comparisons between vertical motions obtained from the quasi-geostrophic omega equation and those in the ECMWF analysis system. ECMWF Technical Memorandum No. 16, pp. 32

Kanamitsu, M. 1980 Some climatalogical and energy budget calculations using the FGGE IIIb analyses during January 1979. Seminars on Data Assimilation Methods, ECMWF, pp. 399-454

Leith, C.E. 1980 Non-linear normal mode initialization and quasi-geotrophic theory. J. Atm. Sci., 37, 958-968

Newell, R.E., Kidson, J.W., Vincent, D.G. and Boer, G.Y. 1972 The general circulation of the tropical atmosphere and interactions with extra-tropical latitudes. Vol. I, The MIT Press, Mass., USA, 258 pp.

Oort, A.H. and Rasmusson, E.M. 1971 Atmospheric Circulation Statistics. NOAA Prof. Paper No. 5, pp. 323

Rosen, R.D. and Salstein, D.A. 1980 A comparison between circulation statistics computed from conventional data and NMC Hough analyses. Mon. Wea. Rev., 108, 1226-1247

Temperton, C. 1980 Design of the ECMWF normal mode initialization procedure. Seminar : Data Assimilation Methods, ECMWF, pp. 159-193

Temperton, C and Williamson, C.L. 1979 Normal mode initialization for a multi-level gridpoint model. ECMWF Technical Report No. 11

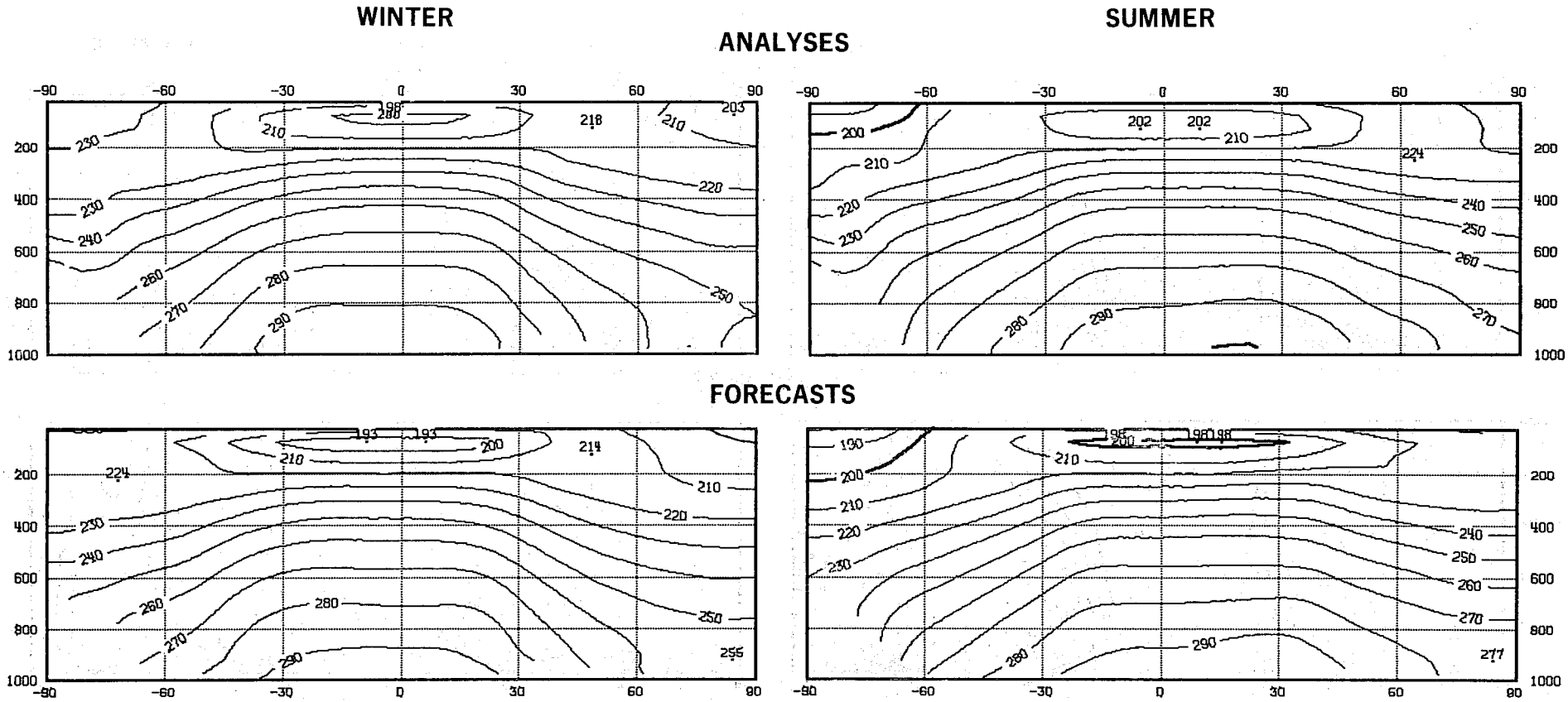

Fig. 1 Cross sections of the zonally averaged mean temperature $[\bar{T}]$ in ^{o}K obtained from ECMWF initialized 12 GMT global operational analyses and forecasts for day 10 for the 1979-1980 winter and 1980 summer.

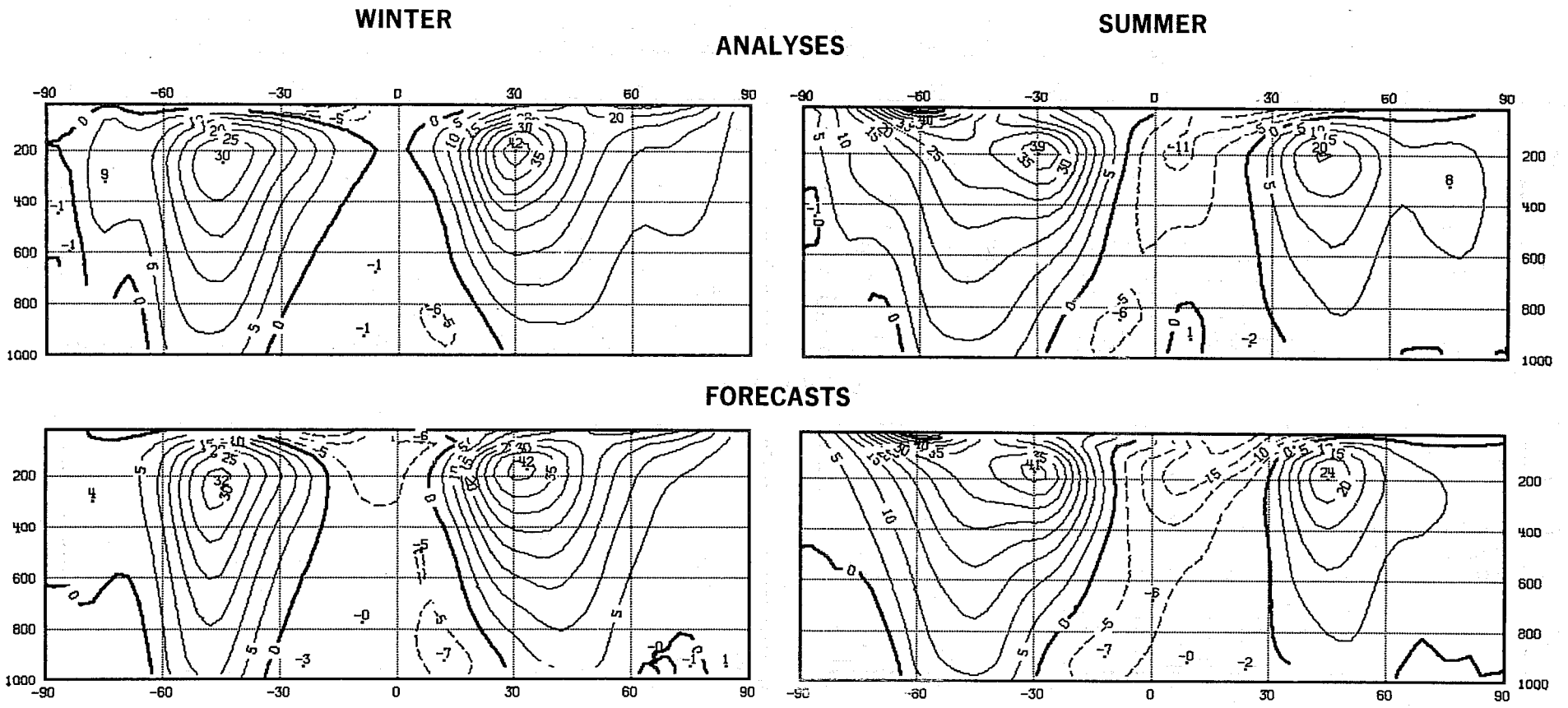

Fig. 2 As Fig. 1 but for zonally averaged mean zonal wind $[\bar{u}]$ in m/s.

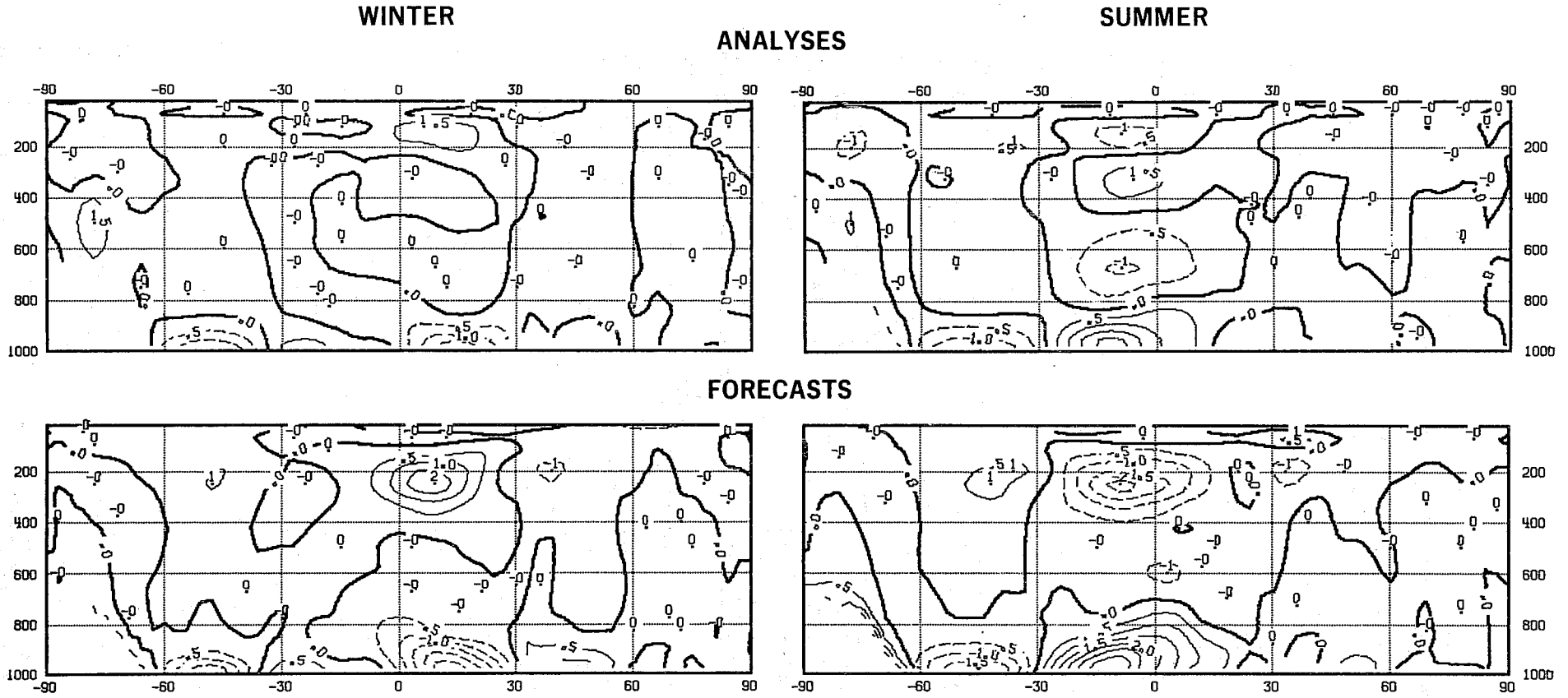

Fig. 3 As Fig. 1 but for zonally averaged mean meridional wind $[\bar{v}]$ in m/s.

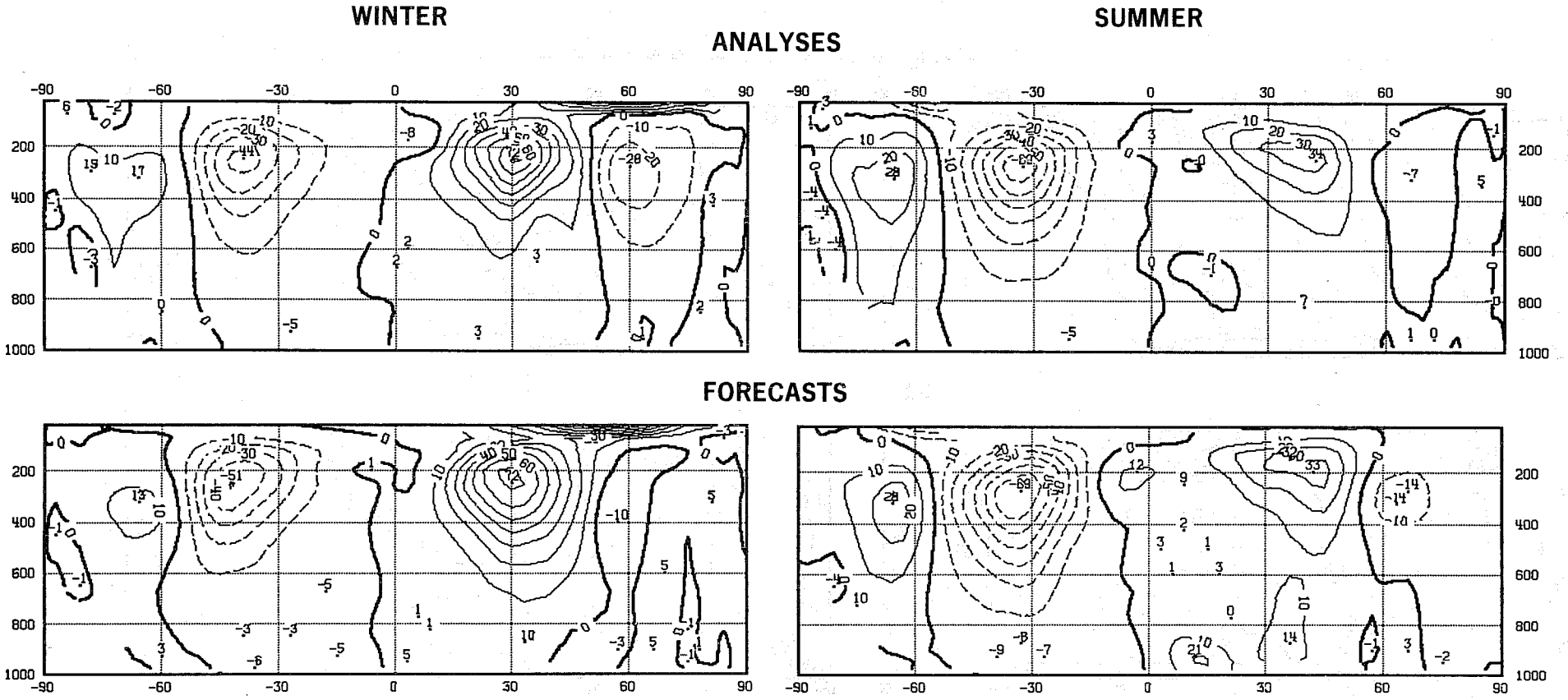

Fig. 4 As Fig. 1 but for total eddy meridional relative angular momentum flux $[\bar{u}^* \bar{v}^*] + [\overline{u'v'}]$ in m^2/s^2.

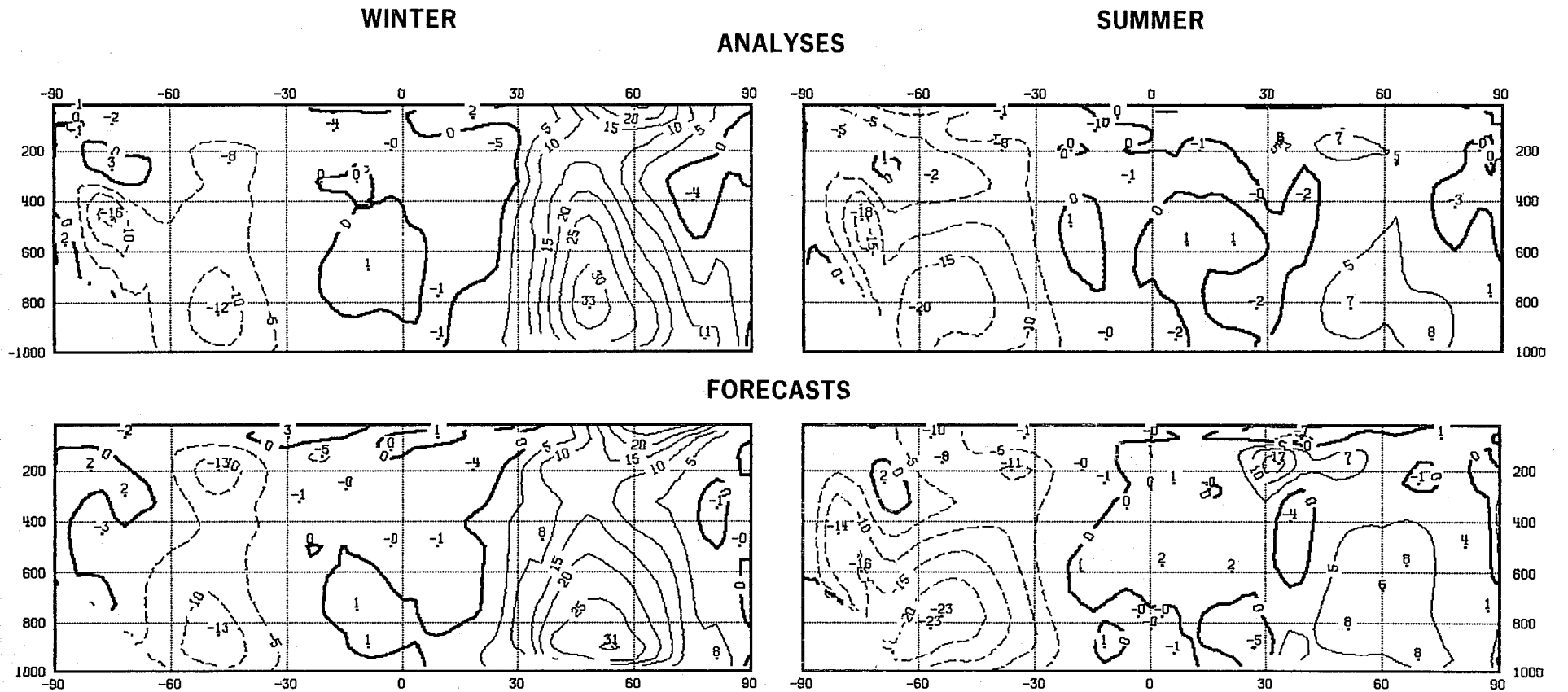

Fig. 5 As Fig. 1 but for total eddy meridional heat flux $[\bar{T}^* \bar{v}^*] + [\overline{T'v'}]$ in ^{o}K m/s.

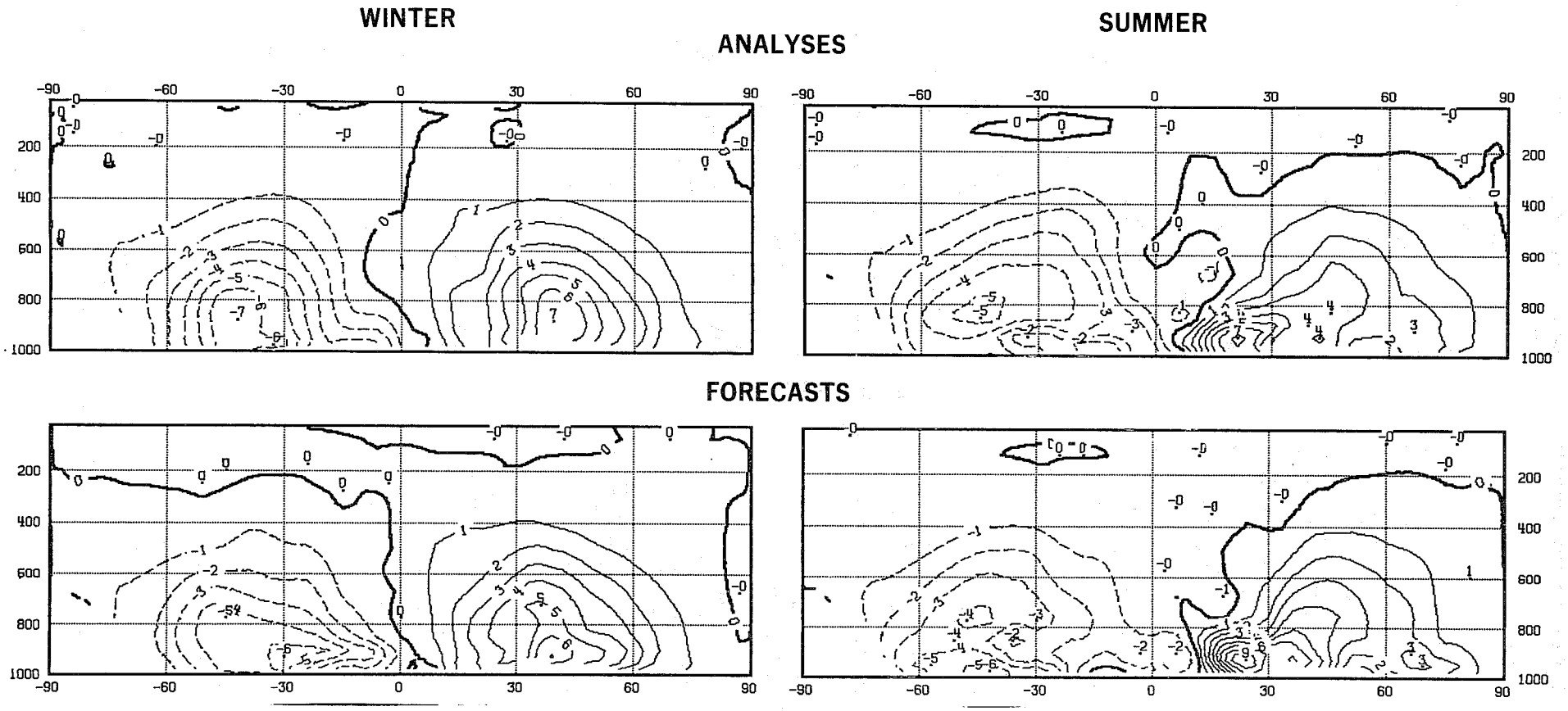

Fig. 6 As Fig. 1 but for total eddy meridional moisture flux $[\bar{q}^* \bar{v}^*] + [\overline{q'v'}]$ in g/kg m/s.

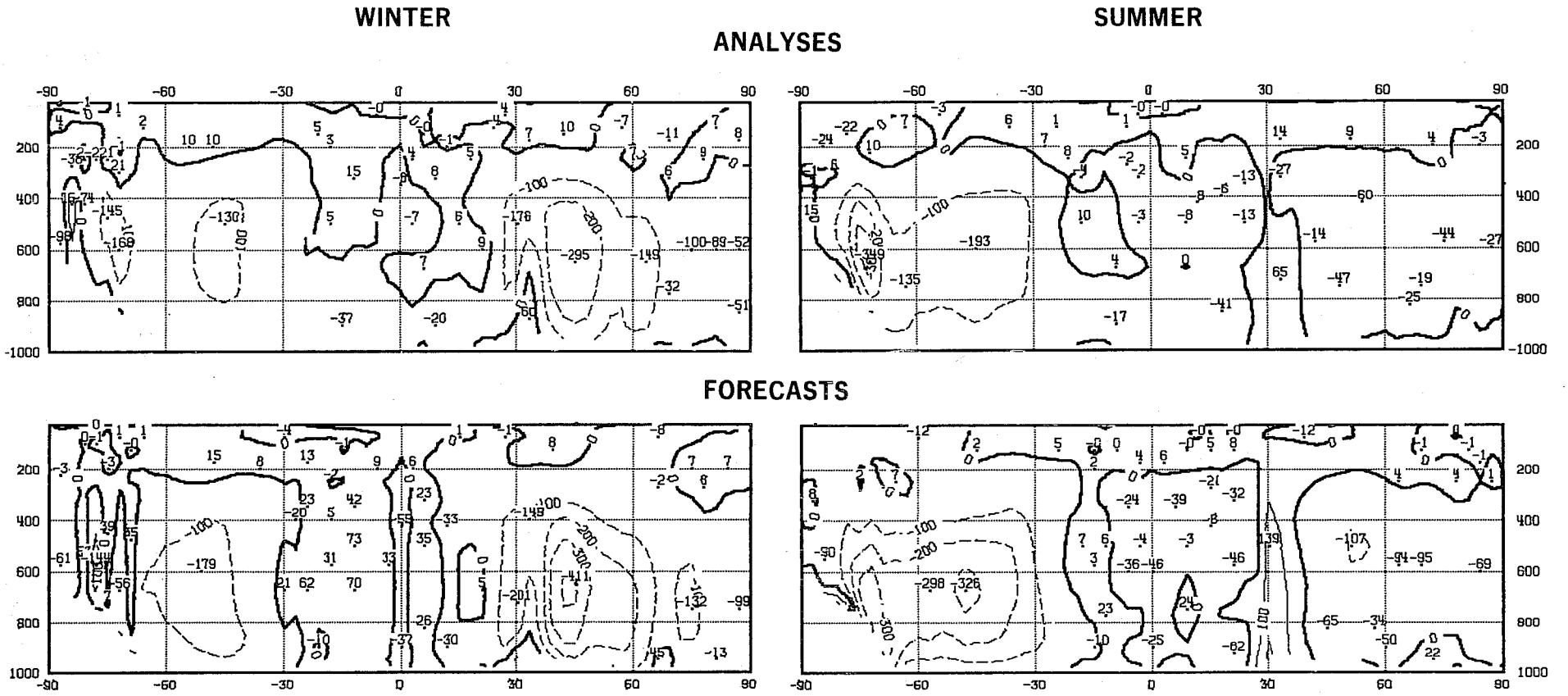

Fig. 7 As Fig. 1 but for total eddy vertical heat flux $[\bar{T}^*\bar{\omega}^*] + [\overline{T'\omega'}]$ in ^{o}K mPa/s.

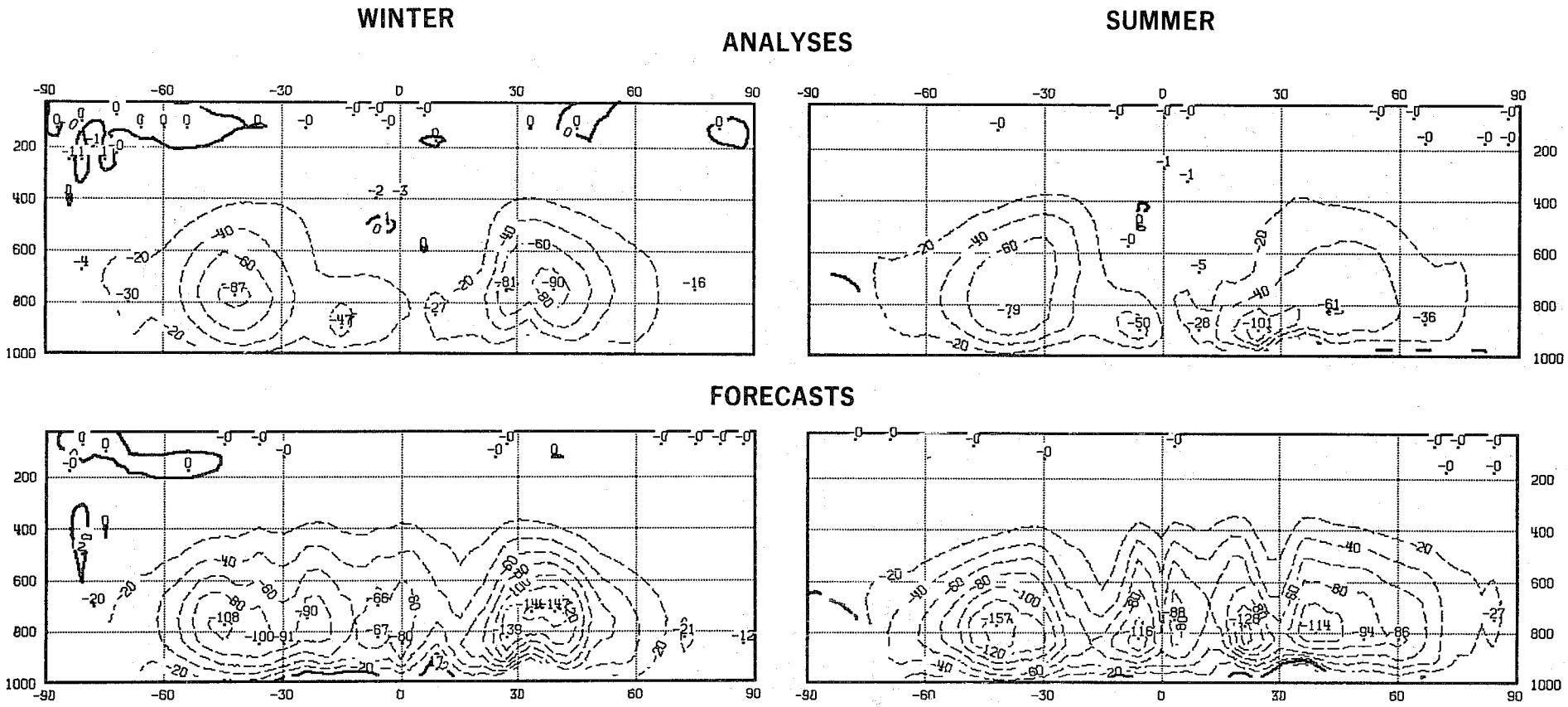

Fig. 8 As Fig. 1 but for total eddy vertical moisture flux $[\bar{q}^* \bar{\omega}^*] + [\overline{q'\omega'}]$ in g/kg mPa/s.

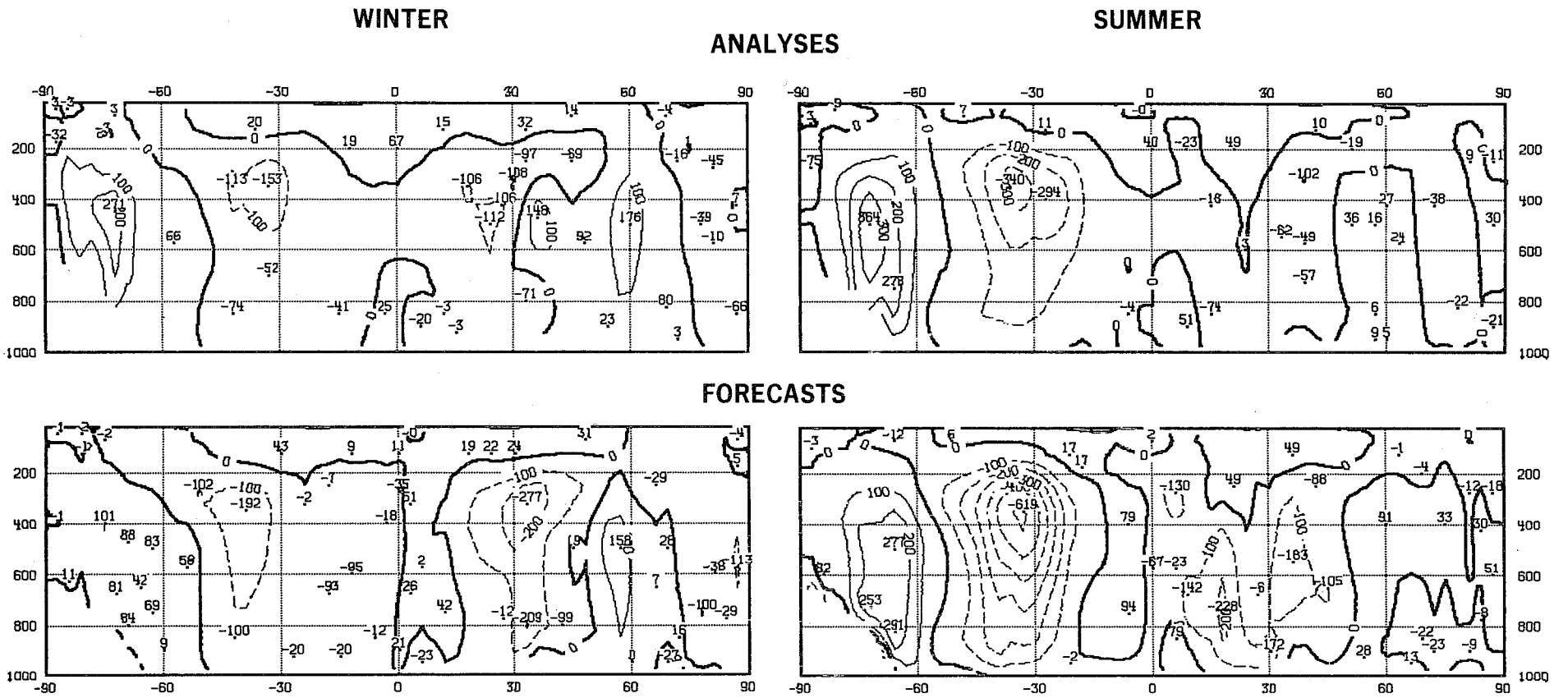

Fig. 9 As Fig. 1 but for total eddy vertical momentum flux $[\bar{u}^*\bar{\omega}^*] + [\overline{u'\omega'}]$ in m/s mPa/s.